Investigation of the DSMC Approach for Ion/neutral Species in Modeling Low Pressure Plasma Reactor

Hao Deng[a], Z. Li[a], D. Levin[a], and L. Gochberg[b]

[a]*Department of Aerospace Engineering, The Pennsylvania State University, University Park, PA 16802-1441*
[b]*The Gochberg Group, Latham, NY 12110-4726*

Abstract. Low pressure plasma reactors are important tools for ionized metal physical vapor deposition (IMPVD), a semiconductor plasma processing technology that is increasingly being applied to deposit Cu seed layers on semiconductor surfaces of trenches and vias with the high aspect ratio (e.g., > 5:1). A large fraction of ionized atoms produced by the IMPVD process leads to an anisotropic deposition flux towards the substrate, a feature which is critical for attaining a void-free and uniform fill. Modeling such devices is challenging due to their high plasma density, reactive environment, but low gas pressure. A modular code developed by the Computational Optical and Discharge Physics Group, the Hybrid Plasma Equipment Model (HPEM), has been successfully applied to the numerical investigations of IMPVD by modeling a hollow cathode magnetron (HCM) device. However, as the development of semiconductor devices progresses towards the lower pressure regime (e.g., < 5 mTorr), the breakdown of the continuum assumption limits the application of the fluid model in HPEM and suggests the incorporation of the kinetic method, such as the direct simulation Monte Carlo (DSMC), in the plasma simulation.

The DSMC method, which solves the Boltzmann equation of transport, has been successfully applied in modeling micro-fluidic flows in MEMS devices with low Reynolds numbers, a feature shared with the HCM. Modeling of the basic physical and chemical processes for ion/neutral species in plasma have been developed and implemented in DSMC, which include ion particle motion due to the Lorentz force, electron impact reactions, charge exchange reactions, and charge recombination at the surface. The heating of neutrals due to collisions with ions and the heating of ions due to the electrostatic field will be shown to be captured by the DSMC simulations. In this work, DSMC calculations were coupled with the modules from HPEM so that the plasma can be self-consistently solved. Differences in the Ar results, the dominant species in the reactor, produced by the DSMC-HPEM coupled simulation will be shown in comparison with the original HPEM results. The effects of the DSMC calculations for ion/neutral species on HPEM plasma simulation will be further analyzed.

Keywords: DSMC, kinetic method, low pressure plasma

INTRODUCTION

The development of the microelectronic devices is enabled by the advancing of the plasma material process technologies. Many steps from the semiconductor fabrication processes utilize the unique features provided by plasma. Currently low pressure, high plasma density reactors, such as the hollow cathode magnetron (HCM), are favored tools for the ionized metal physical vapor deposition (IMPVD) [1, 2], a semiconductor plasma processing technology that is increasingly being applied to deposit Cu seed layers on semiconductor surfaces of trenches and vias with high aspect ratio (*e.g.* $\geq$ 5:1). A large fraction of ionized atoms produced by the IMPVD process leads to an anisotropic deposition flux towards the substrate, a feature which is critical for attaining a void-free and uniform fill. Modeling such devices is challenging due to their high plasma density, reactive environment, and low pressure [1, 3]. The modular code, hybrid plasma equipment model (HPEM) [4], has been successfully applied to the numerical investigations of IMPVD [1, 5, 6, 7]. However, as the development of plasma devices progresses towards the lower pressure regime (*e.g.*, $\leq$ 5 mTorr), the breakdown of the continuum assumption limits the application of the fluid model in HPEM and suggests the incorporation of the kinetic method, such as the direct simulation Monte Carlo (DSMC), in plasma simulations.

The DSMC method, which solves the Boltzmann equation of transport, has been successfully applied in modeling micro-fluidic flows in Microelectromechanical system (MEMS) devices [8] with low Reynolds number, a feature shared by the HCM. DSMC has also been utilized for the plasma simulations in more closely related studies. Economou and Bartel [9] constructed a self-consistent plasma simulation method that used DSMC for modeling the reactive neutral and ion flow in high density plasma reactors. Focusing on the typically large disparity in concentration between ion species and neutral species in the plasma reactor, Bartel [10] further proposed cell based chemistry model, based on an integral balancing concept, that allows all chemistry, particularly the trace reactions. More recently, Farbar [11] coupled the DSMC with the particle-in-cell (PIC) method where one dimensional simulations were performed to evaluate the electric field created in a re-entry flow and the results were compared to those using the ambipolar assumption. The sharp increase of the computational cost was noted for this method of coupling DSMC with PIC.

Based on these encouraging results, DSMC has been proposed as a fully kinetic method to be integrated into HPEM for modeling the ion/neutral species in order to improve the fidelity of the simulations at low pressure, nonequilibrium conditions. The component of HPEM that we proposed to augment with the DSMC method is the Fluid Kinetic Module (FKM) [4], which solves the continuity, momentum, and energy equations for heavy particles, *i.e.*, neutrals and ions. The detailed descriptions on the HCM device and the operating conditions of a benchmark case will be given in the next section, followed by the descriptions on the models employed and newly developed in DSMC for the plasma simulation together with the scheme to couple the DSMC and HPEM calculations. Comparisons between the DSMC-HPEM coupled simulation and the original HPEM results will be discussed in the result section. The conclusion of this work is in the end.

DEVICE AND BENCHMARK CASE

Our numerical investigation simulates a Novellus Systems 200 mm HCM reactor. [12] The schematic of the 2-D axisymmetrical reactor is shown in Fig. 1 (a). Gas is injected through the circular nozzle on the sidewall and exits through a pump port that surrounds the substrate. The HCM includes permanent magnets at the side and at the top of the cup-shaped target, and an electromagnetic below them. The magnetic field, shown in Fig. 1 (b), is constructed in such a way that inside the hollow cathode the magnetic lines are oriented parallel to the vertical sidewall. Together with the strong electrostatic field in the sheath region, a closed $E \times B$ drift is created, which results in an effective confinement for electrons and ions within the hollow cathode. In addition, the secondary electrons that move in circular motion with small Larmor radius near the target surface are also captured by the magnetic field and create additional ionization of the heavy particle species atoms. As the result, a high density plasma can be generated by the HCM reactor. Lastly, for the IMPVD process to work, the metal material for deposition, *e.g.*, Cu, is used as the target surface.

The HPEM code is used to run the HCM plasma simulation first. The baseline case [1] has an Ar inlet flow rate of 250 sccm (standard cubic centimeter per minute), a pressure of 10 mTorr, and power deposition of 10 kW. The detailed inlet jet conditions are listed in Table 1. At the current stage of our work, to simplify the plasma simulation, the modeling of the Cu sputtering in the IMPVD process is not activated. In other words, the HCM device is simulated as a reactor that only generates Ar plasma, *i.e.*, the system includes only three heavy particle species where are Ar, Ar^* (excited state), and Ar^+. The reactions modeled are listed in Table 2. Note that the electron impact (EI) reactions are presently taken from HPEM as source functions to facilitate the comparison between results from HPEM and DSMC-HPEM coupled simulations.

DESCRIPTION OF THE DSMC METHOD

A modified DSMC program, Statistical Modeling in Low-density Environment (SMILE)[13] is used in this research. In the DSMC method[14], the Boltzmann equation of transport for heavy particles is solved exactly if certain numerical requirements are met. The number of real particles that one simulated particle represents, F_{num}, needs to be chosen to ensure that there are more than five simulated particles per cell. Note that based on the previous results from simulations of the IMPVD process, [1] the number densities of the minor species, such as Ar^* and Ar^+, are approximately two orders of magnitude lower than the local number densities of the major species, Ar. Moreover, for the minor species, their number densities are highly non-uniform inside the reactor, and could differ in two orders of magnitude between the maximum and minimum concentration areas. Therefore an appropriate F_{num} must be chosen carefully for DSMC plasma simulations. The criterion in determining the cell size, ΔX, is that it should be in the same order of the mean free path and also meet the spatial resolution requirement. Upon the setting of the cell size, the time step, ΔT, will be chosen so that it takes particles several steps to travel across a cell.

Since only heavy particles are modeled in DSMC, three types of collision are involved in the simulation. First, for heavy-heavy particle collisions, the majorant frequency scheme[15] is employed to calculate the collision frequency. Occurrence of the collision is determined by the variable hard sphere (VHS) model,[14] in which the collision cross section depends on the relative collision velocity, reference value of the collision cross section, and the species viscosity. The Larsen-Borgnakke (L-B) model[16] is used to redistribute the energy between the pair of particles after the collision. Secondly, for collisions between heavy particles and surfaces of the plasma reactor, the Maxwell model with total energy and momentum accommodation is used, with the surface temperature set to be 350 K. In addition, all surfaces are non-stick for Ar, Ar^*, and Ar^+ species, and full charge recombination is assumed when Ar^+ particles hit a surface. Reactive collisions are the third type, which can be further divided into three groups that need to be treated differently. The first reaction in Table 2 is Penning ionization, *i.e.*, heavy particle ionization. Occurrence of the reaction is determined by the total collisional energy (TCE) model [14], and the post-reaction particles undergo the energy redistribution following the L-B model. The next two reactions are identity exchange reactions. The TCE model is used, however, when the reaction occurs, the collision pair simply exchanges particle identities without any

change in energy. In other words, total energy exchange is assumed for these types of reactions. The last three reactions in Table 2 are EI excitation/ionization. The source functions of Ar, Ar^*, and Ar^+ due to the EI reactions are provided by the HPEM calculation in the form of spatially dependent rates. Based on the rates, specific number of Ar particles are changed into Ar^* or Ar^+ in each cell for each time step.

The general flow field condition can be examined through local Knudsen number (K_n) and Reynolds number (R_e) contours. Figure 2 (a) shows that the majority of the area inside the reactor has a K_n that is greater than 0.1. The high local Knudsen number reveals the rarefied flow condition inside the HCM reactor and implies the need for kinetic method in simulation. Figure 2 (b) shows that the Reynolds number remains low throughout the reactor, which indicates that it can take long times for the DSMC flow field to fully reach the steady state. The numerical investigation that employed DSMC to simulate microchannel flows [8] with similar low Reynolds number suggests that with properly chosen numerical parameters, *i.e.*, F_{num}, ΔX, and ΔT, DSMC is capable of modeling the heavy particle species under the challenging flow condition.

In order to model ions in the plasma, their motion under the Lorentz force needs to be solved. In a 2-D axisymmetric case without an external body force, the conventional DSMC simulation keeps track of two coordinates and three velocity components for each particle, and simulates collisions based on the cell information that is assumed to be the properties of particles in a differential shell of the cell thickness. In this work however, the third coordinate for ions also has to be traced, because ions move in a 3-D space under the Lorentz force. The following numerical procedures were implemented to model ions under the effect of the Lorentz force in DSMC . First, the 3-D velocity components of an ion are adjusted according to the local E and B field, and then, the updated 3-D velocity is projected onto the corresponding 2-D axisymmetric coordinate system. Next, the ion particle is moved in 3-D space, and its 2-D axisymmetric coordinates are updated accordingly. In this way, collisions as well as other statistical processes that involve ions can still be calculated properly using the 2-D axisymmetric DSMC procedure. Note that the electrostatic field is also an input to the DSMC simulation from the HPEM results.

The operating pressure is an important parameter for the plasma reactor, therefore a "fictitious" jet is applied at the outlet to meet the given pressure at the pump port. For the effect of the pressure boundary condition to propagate upstream, and also for the interacting processes, such as EI ionizations, acceleration of ions due to the E field, and charge recombination and full accommodation at surfaces, to fully develop throughout the reactor, it becomes critical to make sure that the DSMC simulation runs enough time steps before starting to sample macro-parameters. In this case, the mass conservation of Ar species is chosen as the indicator. The total mass flux of all three Ar related species at the outlet port is calculated and compared with the prescribed inlet jet condition (*e.g.*, 250 sccm corresponds to a flow rate of 1.175×10^{20} $particles/sec$), to determine whether the simulation has reached the steady state. In all DSMC simulations in this work the differences of the flow rates between inlet and outlet are controlled to be within 5%.

The coupling of DSMC and HPEM calculations is achieved through the following scheme. Originally, HPEM solves the mass and momentum conservation equations for ion/neutral species along with the Poisson's equation for electrostatic field using a time step of the nanosecond scale. Electron temperatures and the EI reaction source functions are calculated during the same time. After hundreds of nanoseconds, the energy equations for ion/neutral species and the electron energy distribution function are computed. The HPEM calculation will iterate between these steps until the steady state solution is reached. Now DSMC calculation as a module is inserted into this iteration process to provide HPEM the kinetically solved Ar results. Everytime DSMC calculation is called, it is initialized using the latest results from HPEM, including number densities, temperatures, and velocities of Ar, Ar^*, and Ar^+, EI reaction source functions, and E and B fields. After reaching the steady state, DSMC will then feed back to HPEM the properties of Ar, the dominant species in the reactor.

RESULTS AND DISCUSSION

Note that in order to better show the pattern in comparisons, contours in this section are all self-normalized and use the same scale. Figure 3 shows that DSMC-HPEM coupled simulation predicts a much higher overall Ar number density compared with the original HPEM results. It can be seen in both results that there is a decrease in Ar number density towards the symmetric axis in the bulk region. This is caused by the EI reactions that are stronger in the region close to the symmetric axis and convert Ar particles into either Ar^* or Ar^+. Inside the hollow cathode, especially in the area near the target surface, higher Ar number densities are predicted by DSMC-HPEM coupled simulations. Driven by the strong electrostatic field, there is a strong flux of Ar^+ hitting the target surface, which in turn generates a relatively low velocity Ar flux back from the surface as the result of the full surface accommodation and charge recombination. Figure 4 shows that Ar temperatures in both results have the maximum value inside the hollow cathode, although, the spatial distributions do not agree. The main mechanism that heats up the Ar from the initial injection through the sidewall of the bulk region is the collisions with hot Ar^+ particles which gain energy from the electrostatic field. Therefore in both HPEM and DSMC-HPEM coupled results, the Ar temperature increases as the Ar flow travels

through the bulk region and reaches into the hollow cathode.

As briefly mentioned above, there is a strong electrostatic field near and directed towards the target surface inside the hollow cathode. Meanwhile the E field is in the positive radial direction in general. As a result, the Ar^+ particles accelerate towards surfaces and gain energies along the way. Figure 6 shows that the maximum Ar^+ temperature near the target surface predicted by the coupled simulation is in the same order ($\sim 10^5 K$) as the HPEM results, and is also consistent with the maximum value of the E field ($\sim 10^2 V/cm$) in that region. In the number density comparison, shown in Fig. 5, both results show a Ar^+ concentration on the symmetric axis below the hollow cathode. Near the vertical target surface inside HCM, DSMC-HPEM coupled simulation predicts a larger Ar^+ concentrated region as the result of the EI ionization source functions that are changed by the DSMC calculations.

The frequency in calling the DSMC calculation in the DSMC-HPEM coupled simulation was also investigated. Compared with the DSMC-HPEM coupled simulation shown here in which DSMC is called every 25 HPEM iterations, the one in which DSMC is called every 50 iterations shows the very close steady state results.

CONCLUSIONS

In this work the DSMC calculations are set up to model the heavy particle species and coupled with HPEM to simulate a HCM plasma reactor. Particle collisions, surface collisions, and reactive collisions are included in DSMC. In addition, the Lorentz force on charged particles is modeled based on the electrostatic and magnetostatic field from the HPEM results, and EI reactions are implemented using the source functions from HPEM as input as well. The heating of the neutral species due to collisions with Ar^+ and the heating of Ar^+ due to the electrostatic field are captured by the DSMC method. Ar and Ar^+ number density spatial distributions predicted by the DSMC-HPEM coupled simulation also demonstrate the effect from the EI reactions. Based on the coupled simulation results, it is shown that HPEM is strongly effected by the Ar results from DSMC which leads to changes in its plasma solutions. Further investigation is needed to validate the results.

ACKNOWLEDGMENTS

The authors would like to acknowledge Professor M. Ivanov of the Institute of Theoretical and Applied Mechanics, Russia for the use of the original SMILE code, and the Global Research Consortium (GRC, a subsidiary of the Semiconductor Research Corporation) for their financial support of this research.

REFERENCES

1. V. Vyas, and M. J. Kushner, *Journal of Vacuum Science and Technology A* **24**, 1955–1969 (2006).
2. B. van Schravendijk, S. Kamath, L. Gochberg, and P. van Cleemput, *SEMI technical conference* (1999).
3. D. J. Economou, *Thin Solid Films* **365**, 348–367 (2000).
4. A. Agarwal, *Controlling Activation Energy to Wafers and Walls in Plasma Processing Reactors for Microelectronics Fabrication*, Ph.D. thesis, Department of Chemical Engineering, the University of Illinois at Urbana-Champaign (2007).
5. V. Vyas, *Transport in Low Pressure Plasma Reactors for Materials Processing*, Ph.D. thesis, Department of Materials Science and Engineering, the University of Illinois at Urbana-Champaign (2005).
6. J. Lu, and M. J. Kushner, *Journal of Applied Physics* **87**, 7198–7207 (2000).
7. M. J. Grapperhaus, Z. Krivokapic, and M. J. Kushner, *Journal of Applied Physics* **83**, 35–43 (1998).
8. A. A. Alexeenko, S. F. Gimelshein, and D. A. Levin, *Journal of Microelectromechanical Systems* **14**, 847–856 (2005).
9. D. J. Economou, T. J. Bartel, R. S. Wise, and L. D. P., *IEEE Trans. Plasma Science* **23** (1995).
10. T. J. Bartel, *Rarefied Gas Dynamics: 23rd International Symposium* (2003).
11. E. D. Farbar, and I. D. Boyd, *48th AIAA Science Meeting Including the New Horizons Forum and Aerospace Exposition* (2010).
12. E. Klawuhn, G. C. D'Couto, K. A. Ashtiani, P. Rymer, M. A. Biberger, and K. B. Levy, *Journal of Vacuum Science and Technology A* **18**, 1546–1547 (2000).
13. M. S. Ivanov, G. N. Markelov, and S. F. Gimelshein, *AIAA paper* pp. 1998–2669 (1998).
14. G. A. Bird, *Molecular Gas Dynamics and the Direct Simulation of Gas Flows*, Clarendon Press, Oxford, UK, 1994.
15. M. S. Ivanov, and S. V. Rogasinsky, *Soviet Journal of Numerical Analysis and Mathematical Modeling* **3**, 453–465 (1988).
16. C. Borgnakke, and P. S. Larsen, *Journal of Computational Physics* **18**, 405–420 (1975).

TABLE 1. Gas inlet conditions

Parameter	Ar inlet
(R_1, Z_1), cm	(14.7,10.2)
(R_2, Z_2), cm	(14.7,9.6)
Temperature, K	600
n, cm^{-3}	5.11×10^{13}
Velocity, cm/s	4.15×10^{4}

TABLE 2. Chemical reactions

Reaction	E_a, J	n	A, m^3/s
Ar^*+Ar^* $\rightarrow$ Ar^++Ar+e^-	0.0	0.0	5.0×10^{-16}
Ar+Ar^* $\rightarrow$ Ar^*+Ar	0.0	0.0	1.0×10^{-15}
Ar+Ar^+ $\rightarrow$ Ar^++Ar	0.0	0.0	1.0×10^{-15}
e^-+Ar $\rightarrow$ e^-+Ar^*	-	-	-
e^-+Ar $\rightarrow$ e^-+Ar^++e^-	-	-	-
e^-+Ar^* $\rightarrow$ e^-+Ar^++e^-	-	-	-

(a) (b)

FIGURE 1. (a): HCM device geometry; (b): HCM Magnetic field vectors.

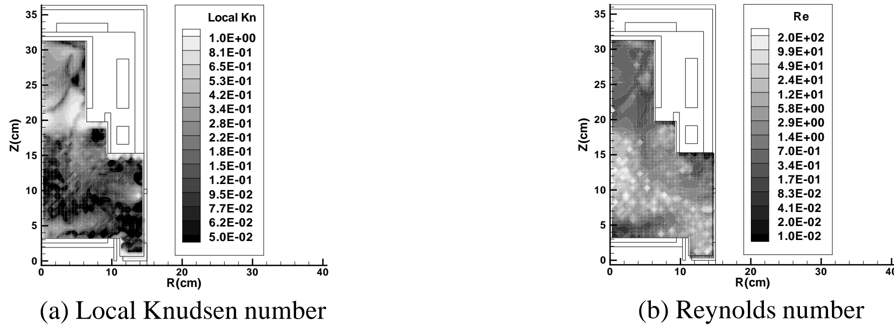

(a) Local Knudsen number (b) Reynolds number

FIGURE 2. General flow field results from DSMC-HPEM coupled simulation.

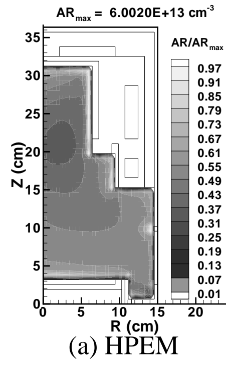

(a) HPEM

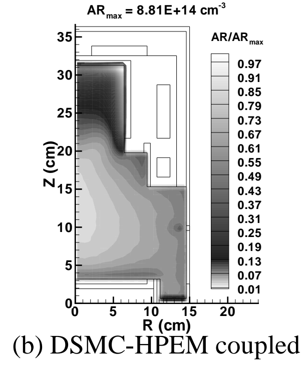

(b) DSMC-HPEM coupled

FIGURE 3. Ar number density comparison.

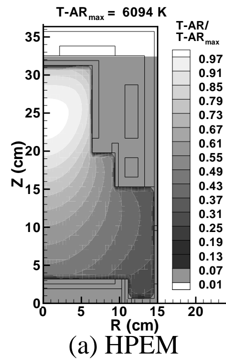

(a) HPEM

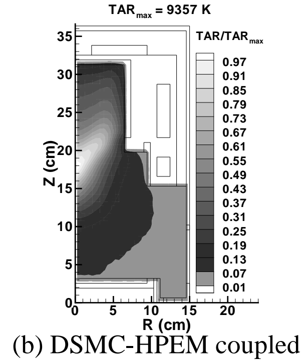

(b) DSMC-HPEM coupled

FIGURE 4. Ar temperature comparison.

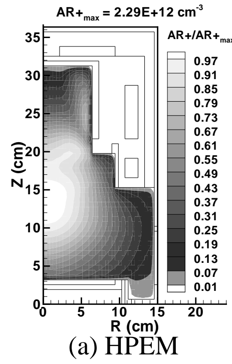

(a) HPEM

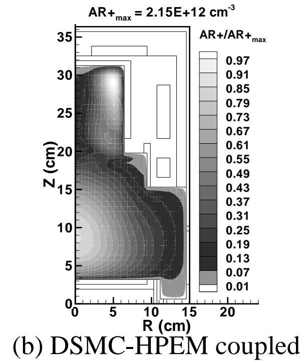

(b) DSMC-HPEM coupled

FIGURE 5. Ar^{+} number density comparison.

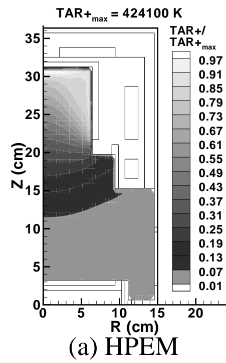

(a) HPEM

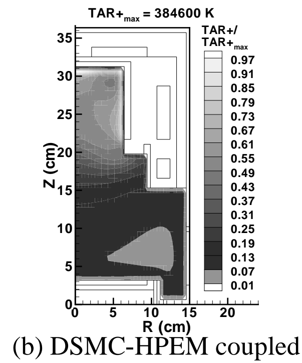

(b) DSMC-HPEM coupled

FIGURE 6. Ar^{+} temperature comparison.